Excitons in quantum dots with parabolic confinement

Weiming Que*
Department of Physics, Simon Fraser University, Burnaby, British Columbia, Canada V5A 1S6
(Received 3 June 1991)

We study excitons in quantum dots with parabolic confining potentials, by solving the electron-hole effective-mass Hamiltonian. We obtain an exact solution for excitons in quantum dots. The exact solution can be obtained in this case because the parabolic form of the confining potential allows the separation of the center-of-mass coordinate and the relative coordinate. The center-of-mass motion of the exciton is a harmonic oscillator. Various approximation methods can now be tested against this exact solution. We compare our exact results with results produced by the configuration-interaction method.

I. INTRODUCTION

The study of low-dimensional systems has received much attention in recent years, especially due to the discovery of such effects as the quantum Hall effect in two-dimensional (2D) systems. The physics in 2D or even lower-dimensional systems presents intriguing challenges both theoretically and experimentally. With the development of modern technology, it is now possible to produce (quasi-)0D systems that confine electrons in all three spatial dimensions. The term "quantum dot" refers to such systems. In the most common usage, it refers to artificially made semiconductor structures using techniques such as etching or grid metal gates.[1] They typically have a disklike shape, a few hundred nanometers in diameter, and a few nanometers thick. In such small structures electron states are quantized into discrete energy levels, with energy spacings of a few meV or more. The same term quantum dot has also been used to refer to semiconductor microcrystallites,[2] which also have the property that the electron states are discretely quantized. Their shape is more like a sphere.

Optical methods are convenient experimental means for studying the properties of quantum-dot systems. They have been used to study various elementary excitations in quantum dots. One type of elementary excitations are collective modes[3] (the analog of plasmons) which have been studied in absorption experiments.[1] Another type of elementary excitations are excitons, which can be created by photons near an absorption edge. They have been the center of attention of many experimentalists ever since the fabrication of quantum dots was made possible. Excitons in quantum dots have been observed in photoluminescence experiments performed on multidot samples,[4] and single-dot samples.[5] On the theoretical side, studies of excitons in microcrystallites have been carried out by variational methods and other approximation methods.[6] Recently a numerical matrix-diagonalization scheme has been used by Hu, Lindberg, and Koch[2] to study excitons in microcrystallites. For excitons in artificially made disklike quantum dots, several theoretical studies have been published.[7,8] The work of Bryant[7] has attracted much attention, who used both variational and configuration-interaction (CI) approaches to calculate the ground-state properties of excitons in quantum dots. Since the problem presented by excitons in quantum dots is in general too complicated for exact solutions, so far no exact solution has been reported in the literature.

In the previous theoretical studies of excitons in quantum dots, a square-well potential has been widely used as the model potential that confines both electrons and holes. The wide use of this model is mostly due to its simplicity. Recent calculations of confining potentials by Kumar, Laux, and Stern[9] show that the confining potential for electrons in a quantum dot can be approximated reasonably well by a parabolic potential. As an interesting theoretical model, we consider quantum dots with parabolic confining potentials for both electrons and holes. The advantage of the model is that it makes an exact solution of the electron-hole effective-mass Hamiltonian possible. Here we present the exact results of this model, and compare to the results by the CI method. The study of this model has been motivated by the exact "generalized Kohn theorem," proved recently by several authors.[10] This paper is a more detailed account of an earlier work[11] on the same topic.

II. EXCITONS IN PARABOLIC QUANTUM DOTS

We start from the effective-mass Hamiltonian for an electron-hole pair in a parabolic quantum dot,

$$H=\sum_i \left[\frac{\mathbf{p}_i^2}{2m_i}+\frac{1}{2}m_i\omega^2\mathbf{r}_i^2\right]-\frac{e^2}{\epsilon|\mathbf{r}_e-\mathbf{r}_h|}\ , \tag{1}$$

where the subscripts e and h represent electron and hole, respectively, $i=e,h$. The second term in (1) produces parabolic confinement. The Coulomb interaction is screened by the background dielectric constant ϵ. Since the first two terms in (1) are both quadratic, and the Coulomb term depends only on the relative coordinate $\mathbf{r}=\mathbf{r}_e-\mathbf{r}_h$, it is not difficult to see that the Hamiltonian is separable in terms of the relative coordinate $\mathbf{r}$ and center-of-mass coordinate $\mathbf{R}$, defined by

$$\mathbf{r}=\mathbf{r}_e-\mathbf{r}_h,\quad \mathbf{R}=\frac{m_e\mathbf{r}_e+m_h\mathbf{r}_h}{M}\ . \tag{2}$$

We also define the total mass $M=m_e+m_h$ and the reduced mass $\mu=m_e m_h/M$. The electron and hole momenta $\mathbf{p}_e$ and $\mathbf{p}_h$ can be expressed in terms of the relative momentum $\mathbf{p}=(\hbar/i)\nabla_{\mathbf{r}}$, and the center-of-mass momentum $\mathbf{P}=(\hbar/i)\nabla_{\mathbf{R}}$, as

$$\mathbf{p}_e=\mathbf{p}+\mathbf{P}\frac{m_e}{M},\quad \mathbf{p}_h=-\mathbf{p}+\mathbf{P}\frac{m_h}{M}\ . \tag{3}$$

Substituting (2) and (3) in the Hamiltonian yields

$$H=\frac{\mathbf{P}^2}{2M}+\tfrac{1}{2}M\omega^2\mathbf{R}^2+\frac{\mathbf{p}^2}{2\mu}+\tfrac{1}{2}\mu\omega^2\mathbf{r}^2-\frac{e^2}{\epsilon|\mathbf{r}|}\ . \tag{4}$$

The explicit separability of the $\mathbf{r}$ and $\mathbf{R}$ coordinates in (4) means that the exciton wave function $\Psi(\mathbf{r}_e,\mathbf{r}_h)$, satisfying the Schrödinger equation

$$H\Psi(\mathbf{r}_e,\mathbf{r}_h)=E\Psi(\mathbf{r}_e,\mathbf{r}_h)\ , \tag{5}$$

can be written as

$$\Psi(\mathbf{r}_e,\mathbf{r}_h)=\chi(\mathbf{R})\phi(\mathbf{r})\ , \tag{6}$$

where $\chi(\mathbf{R})$ is the wave function of a harmonic oscillator. The exciton energy can be written as the sum of the center-of-mass part and the relative motion part, $E=E_{\mathbf{R}}+E_{\mathbf{r}}$. The problem now reduces to solving the relative-motion Hamiltonian

$$H_{\mathbf{r}}=\frac{\mathbf{p}^2}{2\mu}+\tfrac{1}{2}\mu\omega^2\mathbf{r}^2-\frac{e^2}{\epsilon|\mathbf{r}|}\ . \tag{7}$$

Since the second and the third terms in (7) depend on the magnitude of $\mathbf{r}$ only, the angular part of the Hamiltonian is solved trivially. In particular, for the exciton ground state, the wave function depends on $|\mathbf{r}|$ only, (7) gives a 1D differential equation, which we solve numerically by computer.

Quantities of interest include the exciton oscillator strength, and the electron-hole separation. In the envelope-function approximation, the exciton oscillator strength can be written as[7,12]

$$f_{\mathrm{ex}}=\frac{2P^2}{m_0(E_{\mathrm{ex}}-E_0)}\left|\int\Psi(\mathbf{r}_e,\mathbf{r}_e)d\mathbf{r}_e\right|^2\ , \tag{8}$$

where P describes intracell matrix-element effects, m_0 is the bare electron mass, $E_{\mathrm{ex}}-E_0=E+E_g$, and E_g is the optical energy gap. From (6) and (2) we have

$$\Psi(\mathbf{r}_e,\mathbf{r}_e)=\chi(\mathbf{r}_e)\phi(\mathbf{0})\ . \tag{9}$$

Thus (8) can be rewritten as

$$f_{\mathrm{ex}}=\frac{2P^2}{m_0(E_{\mathrm{ex}}-E_0)}|\phi(\mathbf{0})|^2\left|\int\chi(\mathbf{r}_e)d\mathbf{r}_e\right|^2\ . \tag{10}$$

The electron-hole separation r_s in the exciton ground state is defined by $r_s^2=\langle\mathbf{r}^2\rangle$, where the angular brackets denote the expectation value in the ground state.

The Hamiltonian (7) contains two length scales. One is the size of the quantum dot, defined by

$$L=\sqrt{\hbar/\mu\omega}\ . \tag{11}$$

The other length scale is the effective Bohr radius

$$a_B^*=\frac{\epsilon\hbar^2}{\mu e^2}\ . \tag{12}$$

There are also two energy scales. One is the energy quanta due to confinement $\hbar\omega$, which is related to L by

$$\hbar\omega=\frac{\hbar^2}{\mu L^2}\ . \tag{13}$$

The other energy scale is the effective rydberg,[13]

$$\mathcal{R}^*=\frac{e^2}{\epsilon a_B^*}=\frac{\mu e^4}{\epsilon^2\hbar^2}\ . \tag{14}$$

The competition between the two length scales, or equivalently the competition between the two energy scales, defines the strong-confinement regime, where $L\ll a_B^*$, or $\hbar\omega\gg\mathcal{R}^*$, and the weak-confinement regime, where $L\gg a_B^*$, or $\hbar\omega\ll\mathcal{R}^*$.

The above discussion is applicable to both artificilly made disklike quantum dots and semiconductor microcrystallites. In the rest of the paper we concentrate on artificially made disklike quantum dots. Thus the internal motion within quantum dots can be regarded as two dimensional.

It is not the intention of the paper to test all approximation methods used for studying excitons in quantum dots against our exact solution. Here we choose to test the accuracy of the configuration-interaction method of Bryant.[7,14] In the original CI method, the wave functions in the strong-confinement limit are chosen as the basis set, and the Hamiltonian matrix is diagonalized numerically. Since the Hamiltonian matrix is in principle infinite in size, an approximation is made by choosing a finite number of basis states, making the matrix finite. If the exciton ground-state energy changes little when extra basis states are included, the result is then considered to have converged with the chosen number of basis states.

We note that the Hamiltonian (7) can be solved analytically both in the strong- and weak-confinement limits. In the strong-confinement limit where the Coulomb term is neglected, we have a harmonic oscillator. In the weak-confinement limit where the confinement term is neglected, we have a hydrogenic problem. We can therefore choose the wave functions of either limit as the basis set. Each basis set allows the fastest convergence near its appropriate limit. We obtain numerical results by the CI method using both basis sets, and compare to the exact result in Figs. 1 to 3. Before we analyze the numerical results, we spell out the details of both basis sets below.

A. Strong-confinement regime

In the strong-confinement regime, the natural basis set of wave functions are those of the 2D harmonic oscillator. Since the Hamiltonian (7) conserves the azimuthal symmetry, it is advantageous to use polar coordinates rather than Cartesian coordinates. The eigenenergies and eigenstates of a 2D harmonic oscillator in terms of polar coordinates, angular momentum quantum number m, and radial quantum number n are given by

$$E_{nm}=(2n+|m|+1)\hbar\omega \ , \tag{15}$$

$$|n,m\rangle=\frac{1}{\sqrt{2\pi}}e^{im\theta}\left[\frac{2\mu\omega n!}{\hbar(|m|+n)!}\right]^{1/2} \times\rho^{|m|}L_n^{|m|}(\rho^2)e^{-(1/2)\rho^2} \ , \tag{16}$$

where $m=0,\pm1,\pm2,\ldots$, $n=0,1,2,\ldots$, $\rho=r\sqrt{\mu\omega/\hbar}$, and $L_n^{|m|}$ are associated Laguerre polynominals. From (15) we know that the energy is the lowest when $m=0$. Since the full Hamiltonian conserves the azimuthal symmetry, it is diagonal in m. For the ground-state exciton, we only need to consider states with $m=0$. With the basis set (16) we find ($n'\le n$)

$$\langle n',0|H|n,0\rangle=(2n+1)\hbar\omega\delta_{nn'}-\frac{e^2}{\epsilon}\sqrt{\mu\omega/\hbar}\sum_{m=0}^{n'}\frac{(-1)^m n'!}{(n'-m)!(m!)^2 n!}\Gamma(\tfrac{1}{2}+m)\frac{\Gamma(\frac{1}{2}+n-m)}{\Gamma(\frac{1}{2}-m)} \ . \tag{17}$$

Note that $\Gamma(\frac{1}{2}+m)/\Gamma(\frac{1}{2}-m)=(-1)^m[(2m-1)!!]^2/4^m$. From (17) it is clear that the off-diagonal elements will be much smaller than the diagonal ones, provided that

$$\hbar\omega\gg\frac{e^2}{\epsilon}\sqrt{\mu\omega/\hbar} \ . \tag{18}$$

This condition is equivalent to $\hbar\omega\gg\mathcal{R}^*$ or $L\ll a_B^*$. To have a quantitative idea, we calculate $\mathcal{R}^*$ and a_B^* using realistic parameters for GaAs quantum dots: $\epsilon=13.1$, $m_e=0.067m_0$, $m_h=0.09m_0$ (light-hole mass), or $\mu=0.0384m_0$. We obtain $\mathcal{R}^*=6.1$ meV and $a_B^*=18.1$ nm. GaAs quantum dots made today have typically a quantization energy of ~1 meV and a physical lateral size of ~100 nm. The effective size of a quantum dot should be smaller than the physical size because of edge depletion. Comparing these numbers, we conclude that a typical GaAs quantum dot made today is not in the strong-confinement regime defined by (18).

The matrix (17) is a real symmetric matrix. It can be diagonalized numerically, giving us the ground-state energy and wave function. Suppose the ground-state wave function is given by

$$\phi_G=\sum_n a_n|n,0\rangle \ . \tag{19}$$

Using

$$\langle n',0|r^2|n,0\rangle=\frac{\hbar}{\mu\omega}[(2n+1)\delta_{n',n}-(n+1)\delta_{n',n+1} -n\delta_{n',n-1}] \ , \tag{20}$$

we find the electron-hole separation in the ground state to be

$$r_s=L\left[\sum_n[(2n+1)a_n^2-(n+1)a_n a_{n+1}-na_n a_{n-1}]\right]^{1/2} \ . \tag{21}$$

The exciton oscillator strength (10) is related to the center-of-mass wave function $\chi_{nm}(\mathbf{R})$, which is given by replacing μ by M in (16). The integral in (10) is equal to

$$\int\chi_{nm}(\mathbf{R})d\mathbf{R}=(-1)^n2\delta_{m,0}\sqrt{\pi\hbar/M\omega} \ . \tag{22}$$

Using (19) and (16), we find that

$$\phi_G(\mathbf{0})=\sqrt{\mu\omega/\pi\hbar}\sum_n a_n \ . \tag{23}$$

Therefore the oscillator strength for the ground-state exciton is given by

$$f_{\rm ex}=\frac{8P^2}{m_0(E_{\rm ex}-E_0)}\frac{\mu}{M}\left|\sum_n a_n\right|^2 \ . \tag{24}$$

B. Weak-confinement regime

In the weak-confinement regime, the natural basis set of wave functions are those of the 2D hydrogenic problem. The Schrödinger equation for the 2D hydrogenic Hamiltonian $H_0=\mathbf{p}^2/2\mu-e^2/\epsilon r$ is exactly solvable, giving energy eigenvalues and eigen functions[15]

$$E_{nm}=-\frac{\mathcal{R}^*}{2(n+|m|+\frac{1}{2})^2} \ , \tag{25}$$

$$|n,m\rangle=\frac{1}{\sqrt{2\pi}}e^{im\theta}C_{nm}R_{nm}(r), \tag{26a}$$

$$R_{nm}(r)=\rho^{|m|}L_n^{|2m|}(\rho)e^{-\rho/2} \ , \qquad \rho=\frac{2r}{a_B^*(n+|m|+\frac{1}{2})} \ , \tag{26b}$$

$$C_{nm}=\frac{4}{a_B^*}\left[\frac{n!}{(n+2|m|)!(2n+2|m|+1)^3}\right]^{1/2} \ , \tag{26c}$$

where $m=0,\pm1,\pm2,\ldots$, $n=0,1,2,\ldots$. Note that ρ depends on both n and m. Again, since smaller $|m|$ gives lower energy in (25) and the full Hamiltonian conserves the azimuthal symmetry, we only need to consider states with $m=0$ for the ground state. With the basis set (26) we find

$$\langle n',0|r^2|n,0\rangle=a_B^{*2}\frac{(n+\frac{1}{2})^{5/2}}{8(n'+\frac{1}{2})^{3/2}} \times\int_0^\infty dx\,x^3\exp\left[-\frac{x}{2}\left[1+\frac{n+\frac{1}{2}}{n'+\frac{1}{2}}\right]\right] \times L_n(x)L_{n'}\left[\frac{n+\frac{1}{2}}{n'+\frac{1}{2}}x\right] \ . \tag{27}$$

The Hamiltonian matrix is given by

$$\langle n',0|H|n,0\rangle = -\frac{\mathcal{R}^*}{2(n+\frac{1}{2})^2}\delta_{n',n} + \frac{\mu}{2}\omega^2\langle n',0|r^2|n,0\rangle \ . \tag{28}$$

The off-diagonal elements will be much smaller than the diagonal ones provided that

$$\mathcal{R}^* \gg \mu\omega^2 a_B^{*2} = \frac{(\hbar\omega)^2}{\mathcal{R}^*} \ . \tag{29}$$

This condition is equivalent to $\hbar\omega \ll \mathcal{R}^*$, or $L \gg a_B^*$.

The ground-state wave function can again be written in the form $\phi_G = \sum_n a_n|n,0\rangle$, with the ket now representing the basis states (26). The electron-hole separation in the ground state is given by

$$r_S^2 = \sum_{nn'} a_n a_{n'} \langle n',0|r^2|n,0\rangle \ . \tag{30}$$

To calculate the exciton oscillator strength, we find from (26) that $C_{n0} = 4/[a_B^*(2n+1)^{3/2}], R_{n0}(0) = 1$; therefore

$$\phi_G(0) = \frac{4}{a_B^*\sqrt{2\pi}} \sum_n \frac{a_n}{(2n+1)^{3/2}} \ . \tag{31}$$

The oscillator strength for the ground-state exciton is given by

$$f_{\rm ex} = \frac{64P^2}{m_0(E_{\rm ex}-E_0)} \frac{\mu\mathcal{R}^*}{M\hbar\omega} \left| \sum_n \frac{a_n}{(2n+1)^{3/2}} \right|^2 \ . \tag{32}$$

C. Numerical results

Figures 1–3 show the numerical results of the exact solution (solid curves), and the CI method (dashed curves). Figures already presented in the earlier work[11] will not be repeated here. The numerical results of the CI method are obtained by diagonalizing the Hamiltonian matrix with the basis set (16) or (26). In the strong-confinement regime, states with n and n' from 0 to 27 are included, forming a 28×28 Hamiltonian matrix. In the weak-confinement regime, the convergence rate is faster, and states with n and n' from 0 to 22 are included. For comparison, we note that Ref. 2 used 18 states including different angular momentum states, and Ref. 14 used 12 states for square-shaped quantum dots. To produce the figures, we used $m_e = 0.067m_0$, $m_h = 0.09m_0$, $\epsilon = 13.1$, $E_g = 1.51$ eV, and $P^2/m_0 = 1$ eV.[7] These parameters are

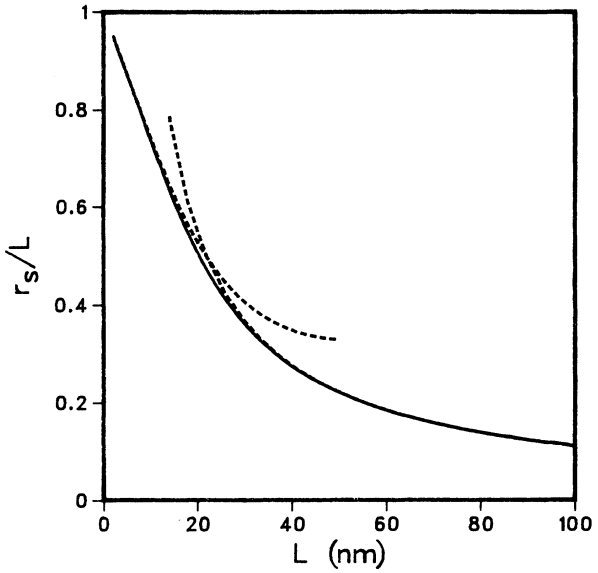

FIG. 2. Electron-hole separation in the exciton ground state. Solid curve, exact result; dashed curves, CI result.

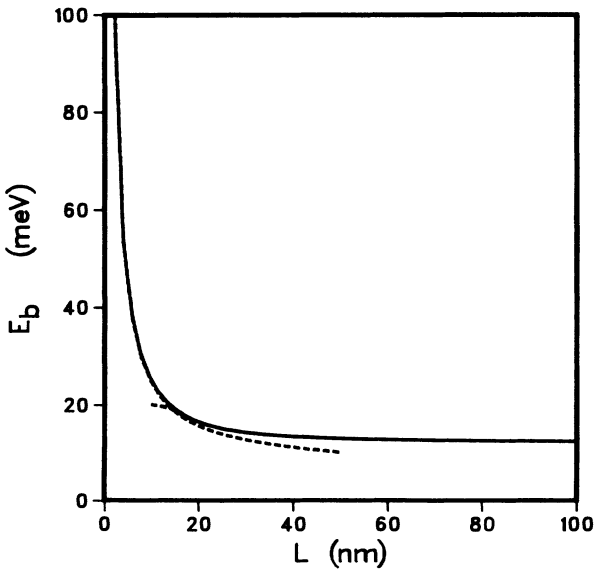

FIG. 1. Exciton ground-state binding energy. Solid curve, exact result; dashed curves, CI result.

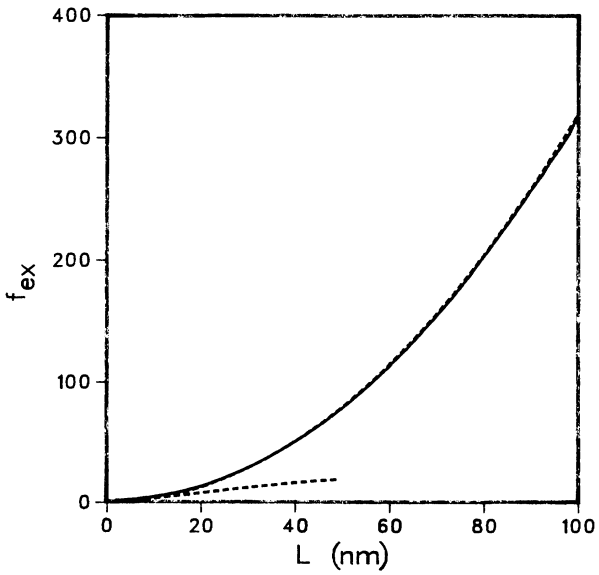

FIG. 3. Oscillator strength for the exciton ground state. Solid curve, exact result; dashed curves, CI result.

realistic for GaAs quantum dots. With these parameter values, the intermediate confinement regime is in the neighborhood of $L \sim a_B^* = 18$ nm.

Figure 1 shows the exciton ground-state binding energy. The binding energy for the ground-state exciton is defined by

$$E_b = \hbar\omega - E \ . \tag{33}$$

The exact solution shows that for $L > 2b$, the binding energy becomes insensitive to the size of the quantum dot. This is an indication of the importance of electron-hole correlation. The CI result using the weak-confinement limit basis set is very accurate for $L \geq 20$ nm. As L decreases, the binding energy increases. In the "strong-confinement approximation,"[2] where correlation between the electron and hole is neglected, E_b becomes zero. Figure 1 shows that this approximation is never realized, because the binding energy increases monotonically as the dot size L decreases. However, in the strong-confinement regime the increase in E_b is slower than the increase in ground-state energy E, because the later is influenced by the faster increase in confinement energy.

Figure 2 shows the electron and hole separation r_s normalized by the dot size L. As L increases from zero, r_s/L decreases from 1. The CI result with the strong-(weak-) confinement basis set is accurate for $L <$ ($>$)20 nm. The exact result can be approximated very well by joining and terminating the two dashed curves at their crossing point.

Figure 3 shows the oscillator strength. The CI result with the weak-confinement basis set almost coincides with the exact result in the figure. This is because for small L where deviation is expected, the magnitude of the oscillator strength itself is small. Experiments are not directly related to f_{ex}, rather to the normalized oscillator strength f_{ex}/L^2. In the plot of f_{ex}/L^2 against L in Ref. 11, it is shown that deviations appear for both basis sets, and for $L < a_B^*$ the normalized oscillator strength is enhanced.

From our results we find that if the strong-confinement basis set is used in the CI method, reasonably accurate exciton energies are obtained with the chosen number of basis states even for $L > a_B^*$. However, for other quantities which depend on the exciton wave function, large errors occur for $L > a_B^*$. This suggests that using the exciton energy only to test convergence can be deceiving, because one can still get large errors for r_s and f_{ex} while the exciton energy has converged. Our results show that instead of using one basis set for the whole range of L, the CI method can produce very good results if two basis sets are used.

III. DISCUSSION

The method used here to obtain exact results works only in a very special case, where the confining potentials for both electrons and holes are parabolic and give the same energy spacings. It does not work in the presence of a magnetic field either. The energy spectra of quantum dots with hard wall and parabolic confining potentials in the presence of a magnetic field have been discussed by Geerinckx, Peeters, and Devreese.[16] In real quantum dots, we expect the confining potentials to deviate from the ideal form assumed here. Thus the method is only useful in the sense that one can use it to test approximate methods for the special case considered here.

In principle, for real quantum dots one should consider the finite thickness of a quantum dot, which is neglected in the calculations of Sec. II. One expects that the finite extent of electron and hole wave functions in the vertical direction will reduce the exciton binding energy. However, corrections due to the finite thickness should be small if the confinement in the vertical direction is very strong.

In conclusion, the effective-mass Hamiltonian for excitons in parabolic quantum dots is solved exactly. The CI method is tested against the exact solution. The parabolic confinement model provides a gauge by which the validity of various approximation methods for excitons in quantum dots can now be verified.

ACKNOWLEDGMENTS

The author would like to thank G. Kirczenow and C. Castaño for useful discussions.

*Present address: Department of Physics, University of Toronto, Toronto, Ontario, Canada M5S 1A7.

[1]M. A. Reed *et al.*, Phys. Rev. Lett. **60**, 535 (1988); Ch. Sikorski and U. Merkt, *ibid.* **62**, 2164 (1989); T. Demel, D. Heitmann, P. Grambow, and K. Ploog, *ibid.* **64**, 788 (1990); J. Alsmeier, E. Batke, and J. P. Kotthaus, Phys. Rev. B **41**, 1699 (1990); A Lorke, J. P. Kotthaus, and K. Ploog, Phys. Rev. Lett. **64**, 2559 (1990).

[2]Y. Z. Hu, M. Lindberg, and S. W. Koch, Phys. Rev. B **42**, 1713 (1990), and references therein.

[3]W. Que and G. Kirczenow, Phys. Rev. B **38**, 3614 (1988).

[4]K. Kash *et al.*, Appl. Phys. Lett. **49**, 1043 (1986); M. A. Reed *et al.*, J. Vac. Sci. Technol. B **4**, 358 (1986); H. Temkin *et al.*, Appl. Phys. Lett. **50**, 413 (1987); Y. Miyamoto *et al.*, Jpn. J. Appl. Phys. **26**, L225 (1987).

[5]K. Kash *et al.* (unpublished).

[6]L. Banyai, Y. Z. Hu, M. Lindberg, and S. W. Koch, Phys. Rev. B **38**, 8142 (1988); T. Takagahara, *ibid.* **39**, 10 206 (1989); S. V. Nair, S. Sinha, and K. C. Rustagi, *ibid.* **35**, 4098 (1987); L. Brus, IEEE J. Quantum Electron. **QE-22**, 1909 (1986), and references therein.

[7]G. W. Bryant, Phys. Rev. B **37**, 8763 (1988); Surf. Sci. **196**, 596 (1988); also in *Interfaces, Quantum Wells, and Superlattices,* edited by R. Taylor and E. W. Fenton (Plenum, New York, 1988).

[8]T. Takejahara, Surf. Sci. **196**, 590 (1988); W. Y. Wu, J. N. Schulman, T. Y. Hsu, and U. Efron, Appl. Phys. Lett. **51**, 710 (1987).

[9]A. Kumar, S. E. Laux, and F. Stern, Phys. Rev. B **42**, 5166 (1990).

[10]L. Brey, N. F. Johnson, and B. I. Halperin, Phys. Rev. B **40** 10 647 (1989); P. A. Maksym and T. Chakraborty, Phys. Rev.

Lett. **65**, 108 (1990); F. M. Peeters, Phys. Rev. B **42**, 1486 (1990).
[11]W. Que, Solid State Commun. **81**, 721 (1992).
[12]C. H. Henry and K. Nassau, Phys. Rev. B **1**, 1628 (1970); E. I. Rashba and G. E. Gurgenishvili, Fiz. Tverd. Tela (Leningrad) **4**, 1029 (1962) [Sov. Phys. Solid State **4**, 759 (1962)].
[13]An unimportant factor of 2 in the denominator in the usual definition of the rydberg has been dropped.
[14]G. W. Bryant, Phys. Rev. Lett. **59**, 1140 (1987).
[15]W. Que (unpublished).
[16]F. Geerinckx, F. M. Peeters, and J. T. Devresse, J. Appl. Phys. **68**, 3435 (1990).